VIP Protein Structures Very Important Paper

DOI: 10.1002/anie.201406357

A Hexameric Peptide Barrel as Building Block of Amyloid-β Protofibrils**

*Christofer Lendel, Morten Bjerring, Anatoly Dubnovitsky, Robert T. Kelly, Andrei Filippov, Oleg N. Antzutkin, Niels Chr. Nielsen, and Torleif Härd**

Abstract: *Oligomeric and protofibrillar aggregates formed by the amyloid-β peptide (Aβ) are believed to be involved in the pathology of Alzheimer's disease. Central to Alzheimer pathology is also the fact that the longer $Aβ_{42}$ peptide is more prone to aggregation than the more prevalent $Aβ_{40}$. Detailed structural studies of Aβ oligomers and protofibrils have been impeded by aggregate heterogeneity and instability. We previously engineered a variant of Aβ that forms stable protofibrils and here we use solid-state NMR spectroscopy and molecular modeling to derive a structural model of these. NMR data are consistent with packing of residues 16 to 42 of Aβ protomers into hexameric barrel-like oligomers within the protofibril. The core of the oligomers consists of all residues of the central and C-terminal hydrophobic regions of Aβ, and hairpin loops extend from the core. The model accounts for why $Aβ_{42}$ forms oligomers and protofibrils more easily than $Aβ_{40}$.*

Alzheimer's disease (AD) is linked to the aggregation and deposition of fibrous amyloid-β (Aβ) peptide into senile plaques in the brain. However, accumulating evidence suggests that the neurodegeneration in AD is associated with soluble prefibrillar oligomers and protofibrils.[1] The relative ratio of the 42-residue $Aβ_{42}$ to the shorter and less aggregation prone $Aβ_{40}$ is also important for the disease mechanism. For instance, an increased $Aβ_{42}$ to $Aβ_{40}$ ratio is associated with familial AD[2] and the formation of neurotoxic aggregates in vitro is critically dependent on this ratio.[3]

The $Aβ_{42}$:$Aβ_{40}$ ratio dependent neurotoxicity can be attributed to distinct biochemical properties and aggregation pathways of the two peptides. $Aβ_{42}$ aggregates more rapidly than $Aβ_{40}$ and can, in particular, more easily form pentameric or hexameric building blocks (paranuclei) that are believed to be the constituents of protofibrils.[4] There is also direct biological evidence for the neurotoxicity of protofibrils. For instance, $Aβ_{42}$ carrying the Arctic mutation (Glu22Gly), which is associated with familial early onset AD, forms protofibrils at a much higher rate than wild-type $Aβ_{42}$.[5] Furthermore, disulfide-linked dimers of $Aβ_{40}$ that carry an Ser26Cys mutation and, unlike wild-type $Aβ_{40}$, very rapidly form protofibrils, are potent inhibitors of hippocampal long-term potentiation, whereas fresh non-protofibrillar preparations of this peptide are not.[6]

Observations of protofibrils of Aβ by electron microscopy[7] and atomic force microscopy[8] were first reported almost two decades ago. Their appearance is polymorphic and depend on aggregation conditions and surfaces.[9,10] Still, typical protofibrils are 5 to 6 nm wide when observed by transmission electron microscopy with negative staining[6,7] and 3 to 5 nm wide when observed by atomic force microscopy (AFM) on mica surfaces.[8,10,11] They are, in general, shorter and more flexible than mature amyloid fibrils, and they frequently appear with curly and beaded features.

Protofibrils of wild-type Aβ are inherently unstable and ultimately form amyloid fibrils. This property has impeded detailed structural studies. We have addressed the issue of protofibril instability by engineering a variant of Aβ (called Aβcc) that forms oligomers and protofibrils, but cannot form amyloid fibrils. Briefly, in Aβcc, alanine residues at positions 21 and 30 are replaced by cysteines, so that a disulfide bond locks the peptide in a conformation that is incompatible with fibril formation and aggregation and is therefore arrested at the protofibril state.[11,12] Protofibrils formed by $Aβ_{42}$cc are

[*] Dr. C. Lendel, Dr. A. Dubnovitsky, Prof. Dr. T. Härd
Department of Chemistry and Biotechnology
Swedish University of Agricultural Sciences (SLU)
Box 7015, SE-750 07 Uppsala (Sweden)
E-mail: Torleif.Hard@slu.se

Dr. M. Bjerring, Prof. Dr. N. C. Nielsen
Center for Insoluble Protein Structures (inSPIN)
Interdisciplinary Nanoscience Center (iNANO) and
Department of Chemistry, Aarhus University
Aarhus (Denmark)

R. T. Kelly, Prof. Dr. O. N. Antzutkin
Department of Physics, Warwick University
Coventry (United Kingdom)

Dr. A. Filippov, Prof. Dr. O. N. Antzutkin
Chemistry of Interfaces, Luleå University of Technology
Luleå (Sweden)

Dr. A. Dubnovitsky
Present address: Department of Clinical Neuroscience, Center for Molecular Medicine, Karolinska Institutet
Stockholm (Sweden)

[**] This work was supported by grants from the Swedish Research Council (VR 621-2011-5812), the Danish National Research Foundation (DNRF59), and the Swedish Alzheimer Foundation (Nr. 10-03-100 and Nr. 12-03-119). Molecular modeling was performed using resources provided by the Swedish National Infrastructure for Computing (SNIC) at NSC, Linköping, Sweden. NMR analyses of synthetic peptides were performed using resources provided by the UK 850 MHz solid-state NMR facility at Warwick, UK. We thank Dr. Ingemar André (Lund University), Dr. Evalena Anderson (SLU), Dr. Joakim Bergström (Uppsala University), and Dr. Sergij Afonin for their assistance.

Supporting information for this article is available on the WWW under http://dx.doi.org/10.1002/anie.201406357.

indistinguishable from wild-type $A\beta_{42}$ protofibrils with respect to many properties: size and morphology as observed by electron microscopy and atomic force microscopy; binding of conformation-specific antibodies and the ANS dye; circular dichroism and infrared spectra; the ability to induce apoptosis in neuroblastoma cell lines; and the ability to attenuate spontaneous synaptic activity in primary neurons.[11,12] Here we use solid-state NMR spectroscopy to study the conformation and packing of the $A\beta_{42}$cc peptide in the protofibrils.

The final step of the purification of recombinantly produced $A\beta_{42}$cc provides monomeric peptides in denaturing guanidinium hydrochloride solution. Protofibrils then form spontaneously upon renaturation in native buffer during size exclusion chromatography or by dialysis. AFM of these aggregates shows rod-like particles of 60–200 nm in length and with a z height of 3.1 ± 0.2 nm.[11] The protofibrils are very stable over time but can, for instance in the presence of SDS, be fragmented into smaller units that appear as dimers and trimers in SDS-PAGE.[12]

Solid-state NMR experiments were performed on lyophilized and rehydrated $A\beta_{42}$cc protofibril samples. Resonances appear with the same chemical shifts in an NMR spectrum of a sample prepared by sedimentation (see the Supporting Information, Figure S1). ^{13}C–^{13}C correlation spectra of a sample of uniformly ^{13}C,^{15}N-labeled peptide (Figure 1a) show well-separated ^{13}C resonances with line widths of 1.0 to 1.5 ppm, indicating the presence of well-defined structural elements. Furthermore, only one set of resonances is observed, indicating that $A\beta_{42}$cc adopts a single conformation in the protofibrils.

The ^{13}C–^{15}N correlation spectrum displays a number of distinguishing sharp resonances (Figure S2). These were assigned to a C-terminal fragment of the peptide. 97% of the ^{13}C and ^{15}N resonances of residues 31–42 were assigned (Table S1) and secondary chemical shifts indicate extended β-strand conformation of this fragment (Figure 1b). Partial assignments (52% of all ^{13}C and ^{15}N atoms; Table S1) of the segment between residues 15 and 30 were aided by the use of two synthetic peptide samples with uniform ^{13}C- and ^{15}N-labeling of selected residues (see the Supporting Information, Figure S1).

Secondary chemical shifts suggest that residues 17–20 also adopt a β-strand conformation, while the region around residues 25 and 26 has a less defined secondary structure (Figure 1b). In addition, connectivities between one or more phenylalanine (Phe19 and/or Phe20) and isoleucine (Ile31, Ile32 and/or Ile41) side chains in ^{13}C–^{13}C correlation spectra (Figure S3) are in agreement with a β-hairpin conformation of the two β strands.

A second NMR sample of recombinant protofibrils was produced from a 1:1 mixture of ^{15}N- and ^{13}C-labeled peptides. This sample was used to record ^{13}C–^{15}N PAIN (proton-assisted insensitive nuclei cross polarization) correlation data[13] to detect intermolecular NMR connectivities. The majority of the correlations in the PAIN spectrum were assigned as connectivities between C-terminal residues (Figure 1c, Figure S3, and Table S2).

Hence, the NMR data support the presence of a β hairpin and a C-terminal β strand in $A\beta_{42}$cc protomers, and protomer packing involving interactions between nonpolar residues in the central and C-terminal peptide fragments. We used NMR data and the Rosetta molecular modeling software[14] to model the topology and packing of $A\beta_{42}$cc (residues 15–42) in protofibrils at two independent levels. First, we modeled the conformation of single peptide protomers using NMR chemical shifts and restraints based on intramolecular connectivities (Table S3) and, second, we included intermolecular NMR restraints (Table S2) to model an oligomeric building block of the protofibrils.

The protomer model is shown in Figure S4. The topology involves three β strands with connecting turns. Residues 16–36 adopt a β hairpin conformation and residues 39–41 at the C terminus form a third shorter β strand following a turn involving residues 37–38. Similar conformations of the C terminus have been observed in molecular dynamics simulations, and they have been suggested to constitute an important conformational difference between $A\beta_{40}$ and $A\beta_{42}$.[15] The turn at positions 37 and 38 is also present in an $A\beta_{40}$ fibril morphology derived from amyloid in an AD brain.[16]

Next, we modeled the quaternary structure of protofibrils using also intermolecular NMR restraints (Table S2). The protomer structure calculated earlier was not fixed in this modeling. The models were further assumed to be symmetric, because a single set of NMR resonances (see above) indicates a single protomer conformation with identical packing of all protomers. While attempts to build dimers, trimers, or extended fibril-like models were unsuccessful, we found that hexamer models were consistent with the experimental data. It is possible that barrel models with other stoichiometries are also consistent with our NMR data. However, evidence from other experiments also support a hexameric stoichiometry. For instance, chemical cross-linking has previously been used to show that pentameric and/or hexameric assemblies (so-called paranuclei) precede the aggregation of $A\beta_{42}$ (but not $A\beta_{40}$) into protofibrils.[4] Moreover, ion mobility mass spectrometry suggests that $A\beta_{42}$ forms both hexamers and dodecamers, but not octamers.[17] Hexameric building blocks in $A\beta_{42}$cc protofibrils are also in agreement with AFM data (see the Supporting Information for details).

Our final hexamer model is shown in Figure 2. It is a barrel with six-fold cylindrical symmetry in which protomers pack to form a large common hydrophobic core at one end of the barrel. The core involves all nonpolar residues of the hydrophobic C terminus and parts of the side chains in the central KLVFF motif. The β hairpin loops then extend from the core to form the other end of the barrel. Interestingly, the topology allows the short C-terminal β strand to interact with residues 34–36 in the adjacent protomer (Figure 2c). Several facts support this model: 1) it is consistent with experimental data (with no restraint violation larger than 0.7 Å and a root-mean-square (r.m.s.) restraint violation of 0.14 Å); 2) the Rosetta score is favorable (−113; distance restraints not included), thus indicating that this is a physically reasonable model; 3) the approximately 40% extended strand conformation of the backbone is consistent with the circular

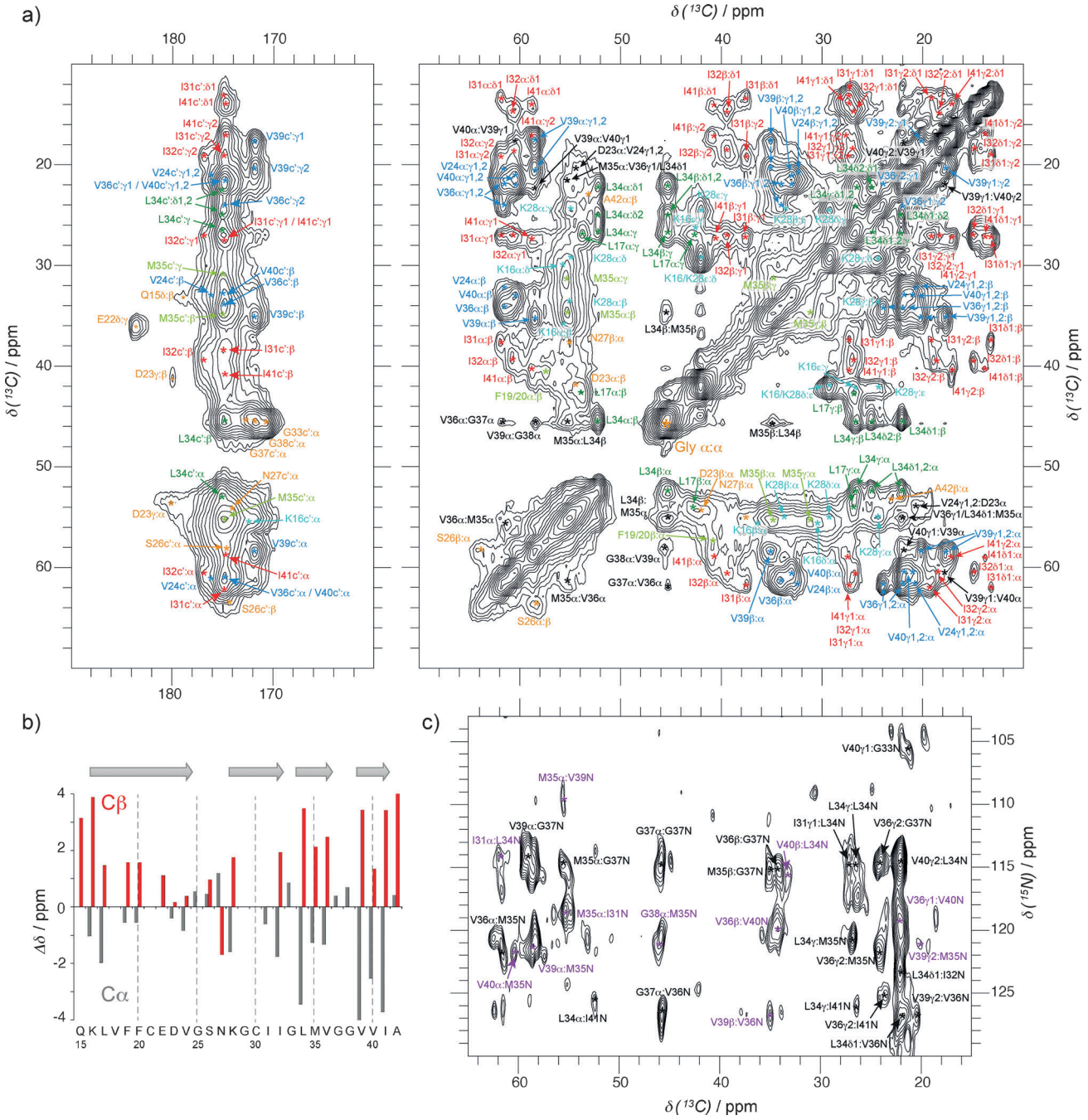

Figure 1. Solid-state NMR data of $A\beta_{42}$cc protofibrils. a) ^{13}C–^{13}C DARR (dipolar-assisted rotational resonance) correlation spectrum of uniformly ^{13}C,^{15}N-labeled protofibrils recorded with 50 ms mixing time. Coloring of assignments reflects different categories of amino acid residues; assignments in black indicate inter-residue correlations. b) Secondary Cα (grey) and Cβ (red) chemical shifts[26] in the fragment 15–42. The positions of β strands in the final hexamer model are indicated. c) ^{13}C–^{15}N PAIN correlation NMR spectrum of protofibrils prepared from a 1:1 mixture of ^{13}C- and ^{15}N-labeled $A\beta_{42}$cc. The final assignments are indicated. Correlations that are unique to $A\beta_{42}$cc protofibrils and incompatible with the structures of Aβ amyloid fibrils are shown in purple (see the Supporting Information and Table S4).

dichroism spectrum of β-sheet oligomers of $A\beta_{42}$cc;[12] and 4) the length and outer diameter of the barrel (2.7 to 3.3 nm) is in agreement with the AFM *z* height[11] (though residues 1–14 are not accounted for in the model, and are perhaps also not visible in AFM).

The hexamer barrel that we propose accounts for several biochemical observations of Aβ aggregation. Most important, the C-terminal Ile41 and Ala42 are part of the hydrophobic core and therefore most likely act to stabilize the barrel (Figure 2c). This would account for more rapid aggregation of $A\beta_{42}$ compared to $A\beta_{40}$[18] and also explain why $A\beta_{40}$

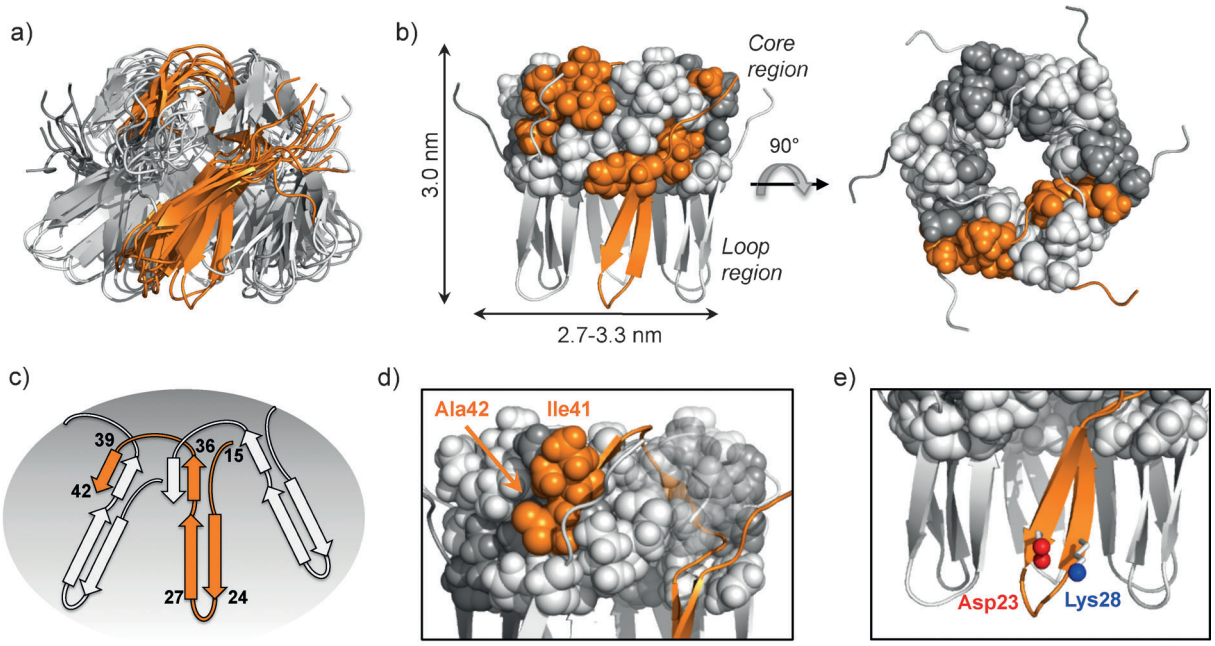

Figure 2. Models of hexameric $A\beta_{42}cc$ building blocks of protofibrils. a) Superposition of the ten models with the lowest Rosetta scores (residues 1–14 were not included in the modeling; all-atom r.m.s. deviation = 1.31 Å). b) Dimensions of the hexamer barrel with the loop and core regions indicated. Side chains of the hydrophobic core (those with the largest change in accessible surface area upon hexamer formation) are shown as spheres. The image to the right is rotated by 90° relative to the left image. c) Simplified representation of the hexamer topology. The numbers refer to the residue positions in the orange protomer. d) The backbone and side chains of the C-terminal residues Ile41 and Ala42 (orange spheres) are packed into the hydrophobic core of the hexamer. e) Asp23-Lys28 salt bridge.

assembles into different aggregate intermediates and forms protofibrils less easily.[4] Furthermore, we find that the Asp23 and Lys28 side chains form an intraprotomer salt bridge that stabilizes the hairpin loops (Figure 2e). This interaction was previously postulated to nucleate Aβ monomer folding,[19] and $A\beta_{40}$ with Asp23 and Lys28 linked by a lactam bridge aggregates very rapidly.[20] We also note that the proposed architecture of preglobulomers of Aβ agrees very well with our model.[21] Finally, the face-to-face packing of β hairpins is consistent with the model for the seeding of amyloid fibril formation that was suggested in Ref. [22] (Figures 3 and S5).

We compared NMR chemical shifts of $A\beta_{42}cc$ protofibrils with those of antibody-stabilized protofibrils of $A\beta_{40}$ (Ref. [23]) and smaller oligomers of wild-type $A\beta_{42}$ (Ref. [24]). Correlation plots indicate that these three aggregates share structural similarities that are larger than their similarities to, for instance, AD-brain-derived amyloid fibrils[16] of $A\beta_{40}$ (Figure S6). In particular, it appears that

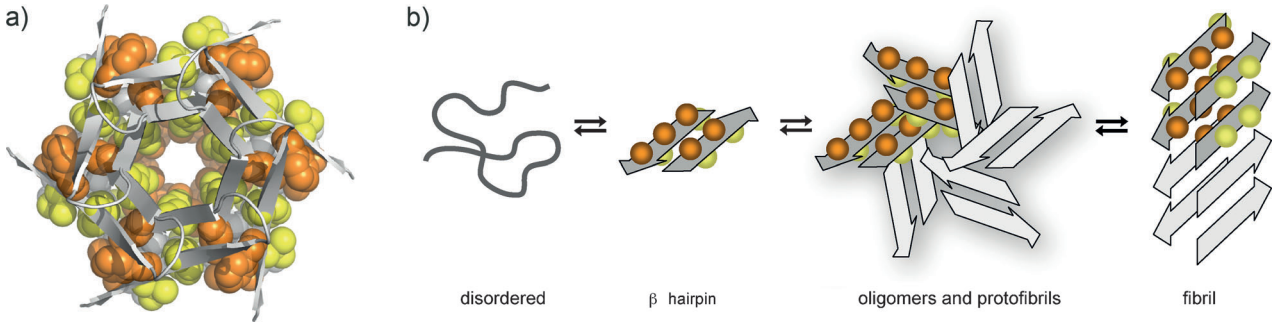

Figure 3. Relation between the $A\beta_{42}cc$ hexamer model and the Aβ aggregation mechanism proposed by Hoyer et al.[22] a) Hexamer barrel oligomer of $A\beta_{42}cc$ in which nonpolar side chains on the two faces of the β-hairpin protomers have been colored yellow and orange, respectively, as in Ref. [22]. Protomer packing involves interactions between yellow side chains on one protomer with orange side chains on a neighboring protomer. b) Schematic of an aggregation mechanism that involves the β hairpin as a transient conformation sampled by monomeric Aβ and as a constituent of Aβ oligomers and protofibrils. Hydrophobic stacking of β hairpins in the hexamer barrel is illustrated schematically. A concerted conformational transition establishes a fibril seed with in-register parallel β sheets. This "Ventian blind" conformational change involves a rotation of hairpin β strands by 90°, so that (orange) side chains previously on one face of the β hairpin now form the hydrophobic core of the fibril seed.[22] The conformational change is inhibited by the double cystein mutation in $A\beta_{42}cc$, which is why aggregation is halted and $A\beta_{42}cc$ forms stable protofibrils.[12] A more detailed illustration is provided in Figure S5.

the conformation of residues 31 to 42 that we observe in protofibrils is present already in smaller $A\beta_{42}$ oligomers. The most important difference between $A\beta_{42}$cc and $A\beta_{40}$ protofibrils is the C-terminal β strand in $A\beta_{42}$cc. This conformation is presumably not supported in $A\beta_{40}$ protofibrils because of a lack of stabilizing interactions at positions 41 and 42, as discussed above.

Ion mobility mass spectrometry detected the formation of $A\beta_{42}$ hexamers and dodecamers, but not 18-mers.[17] Our model explains this observation, because the hexamer model is asymmetric. We explored three potential ways to assemble hexamer barrels into protofibrils: core-to-core, loop-to-loop, and core-to-loop (Figure S7). All three interfaces appear reasonable with the loop-to-loop interface as the best with around 1400 $Å^2$ hidden surface area and a shape complementarity score[25] of 0.83. It might therefore be the interface of the dodecamers observed by mass spectrometry. If this is the case, this interface must be combined with the core-to-core interface to build extended protofibrils (Figure S7). Interestingly, at the loop-to-loop interface Ser26 of neighboring protomers are in close proximity (3.1 Å between the Oγ atoms; Figure S7), which would explain why disulfide-linked dimers formed by $A\beta_{40}$ with a Ser26Cys mutation very easily form toxic protofibrils.[6] The present data does not allow a distinction of packing modes, but it nevertheless establishes oligomeric peptide barrels as likely building blocks in the higher-order assembly of Aβ protofibrils.

Received: June 18, 2014
Revised: August 8, 2014
Published online: September 26, 2014

Keywords: Alzheimer's disease · amyloid β-peptides · neurotoxicity · oligomers · protein structures

[1] a) C. Haass, D. J. Selkoe, *Nat. Rev. Mol. Cell Biol.* **2007**, *8*, 101 – 112; b) P. Lansbury, H. Lashuel, *Nature* **2006**, *443*, 774 – 779.
[2] D. Scheuner, C. Eckman, M. Jensen, X. Song, M. Citron, N. Suzuki, T. Bird, J. Hardy, M. Hutton, W. Kukull, E. Larson, E. Levy-Lahad, M. Viitanen, E. Peskind, P. Poorkaj, G. Schellenberg, R. Tanzi, W. Wasco, L. Lannfelt, D. Selkoe, S. Younkin, *Nat. Med.* **1996**, *2*, 864 – 870.
[3] I. Kuperstein, K. Broersen, I. Benilova, J. Rozenski, W. Jonckheere, M. Debulpaep, A. Vandersteen, I. Segers-Nolten, K. V. D. Werf, V. Subramaniam, D. Braeken, G. Callewaert, C. Bartic, R. D'hooge, I. C. Martins, F. Rousseau, J. Schymkowitz, B. de Strooper, *EMBO J.* **2010**, *29*, 3408 – 3420.
[4] G. Bitan, M. D. Kirkitadze, A. Lomakin, S. S. Vollers, G. B. Benedek, D. B. Teplow, *Proc. Natl. Acad. Sci. USA* **2003**, *100*, 330 – 335.
[5] C. Nilsberth, A. Westlind-Danielsson, C. Eckman, M. M. Condron, K. Axelman, C. Forsell, C. Stenh, J. Luthman, D. B. Teplow, S. Younkin, J. Näslund, L. Lannfelt, *Nat. Neurosci.* **2001**, *4*, 887 – 893.
[6] B. O'Nuallain, D. B. Freir, A. J. Nicoll, E. Risse, N. Ferguson, C. E. Herron, J. Collinge, D. M. Walsh, *J. Neurosci.* **2010**, *30*, 14411 – 14419.
[7] D. Walsh, A. Lomakin, G. Benedek, M. Condron, D. Teplow, *J. Biol. Chem.* **1997**, *272*, 22364 – 22372.
[8] J. Harper, S. Wong, C. Lieber, P. Lansbury, *Chem. Biol.* **1997**, *4*, 119 – 125.
[9] B. Caughey, P. Lansbury, *Annu. Rev. Neurosci.* **2003**, *26*, 267 – 298.
[10] B. Moores, E. Drolle, S. Attwood, J. Simons, Z. Leonenko, *PLoS One* **2011**, *6*, e25954.
[11] A. Dubnovitsky, A. Sandberg, M. M. Rahman, I. Benilova, C. Lendel, T. Härd, *PLoS One* **2013**, *8*, e66101.
[12] A. Sandberg, L. M. Luheshi, S. Söllvander, T. P. de Barros, B. Macao, T. P. Knowles, H. Biverstål, C. Lendel, F. Ekholm-Petterson, A. Dubnovitsky, L. Lannfelt, C. M. Dobson, T. Härd, *Proc. Natl. Acad. Sci. USA* **2010**, *107*, 15595 – 15600.
[13] J. R. Lewandowski, G. De Paepe, R. G. Griffin, *J. Am. Chem. Soc.* **2007**, *129*, 728 – 729.
[14] A. Leaver-Fay, M. Tyka, S. Lewis, O. Lange, J. Thompson, R. Jacak, K. Kaufman, P. Renfrew, C. Smith, W. Sheffler, I. Davis, S. Cooper, A. Treuille, D. Mandell, F. Richter, Y.-E. A. Ban, S. Fleishman, J. Corn, D. Kim, S. Lyskov, M. Berrondo, S. Mentzer, Z. Popović, J. Havranek, J. Karanicolas, R. Das, J. Meiler, T. Kortemme, J. Gray, B. Kuhlman, D. Baker, P. Bradley, *Methods Enzymol.* **2011**, *487*, 545 – 574.
[15] a) B. Urbanc, L. Cruz, S. Yun, S. V. Buldyrev, G. Bitan, D. B. Teplow, H. E. Stanley, *Proc. Natl. Acad. Sci. USA* **2004**, *101*, 17345 – 17350; b) D. Rosenman, C. Connors, W. Chen, C. Wang, A. García, *J. Mol. Biol.* **2013**, *425*, 3338 – 3359.
[16] J.-X. Lu, W. Qiang, W.-M. Yau, C. Schwieters, S. Meredith, R. Tycko, *Cell* **2013**, *154*, 1257 – 1268.
[17] S. L. Bernstein, N. F. Dupuis, N. D. Lazo, T. Wyttenbach, M. M. Condron, G. Bitan, D. B. Teplow, J. E. Shea, B. T. Ruotolo, C. V. Robinson, M. T. Bowers, *Nat. Chem.* **2009**, *1*, 326 – 331.
[18] J. Jarrett, E. Berger, P. Lansbury, *Biochemistry* **1993**, *32*, 4693 – 4697.
[19] N. D. Lazo, M. A. Grant, M. C. Condron, A. C. Rigby, D. B. Teplow, *Protein Sci.* **2005**, *14*, 1581 – 1596.
[20] K. Sciarretta, D. Gordon, A. Petkova, R. Tycko, S. Meredith, *Biochemistry* **2005**, *44*, 6003 – 6014.
[21] L. Yu, R. Edalji, J. E. Harlan, T. F. Holzman, A. P. Lopez, B. Labkovsky, H. Hillen, S. Barghorn, U. Ebert, P. L. Richardson, L. Miesbauer, L. Solomon, D. Bartley, K. Walter, R. W. Johnson, P. J. Hajduk, E. T. Olejniczak, *Biochemistry* **2009**, *48*, 1870 – 1877.
[22] W. Hoyer, C. Grönwall, A. Jonsson, S. Ståhl, T. Härd, *Proc. Natl. Acad. Sci. USA* **2008**, *105*, 5099 – 5104.
[23] H. A. Scheidt, I. Morgado, S. Rothemund, D. Huster, M. Fändrich, *Angew. Chem. Int. Ed.* **2011**, *50*, 2837 – 2840; *Angew. Chem.* **2011**, *123*, 2889 – 2892.
[24] M. Ahmed, J. Davis, D. Aucoin, T. Sato, S. Ahuja, S. Aimoto, J. Elliott, W. van Nostrand, S. O. Smith, *Nat. Struct. Mol. Biol.* **2010**, *17*, 561 – 567.
[25] M. Lawrence, P. Colman, *J. Mol. Biol.* **1993**, *234*, 946 – 950.
[26] D. S. Wishart, B. D. Sykes, *J. Biomol. NMR* **1994**, *4*, 171 – 180.

